Effect of accounting for public holidays on skills of atmospheric composition model SILAM v.5.7

Yalda Fatahi[1], Rostislav Kouznetsov[1,2], Mikhail Sofiev[1]

[1]Finnish Meteorological Institute, Helsinki, Finland
[2]AM Obukhoc institute for Atmospheric Physics, Moscow, Russia

Correspondence to: Yalda Fatahi (yalda.fatahi@fmi.fi)

Abstract. The study quantifies the impact of emission changes during public holidays on air quality and analyses the added value of accounting for the holidays in AQ modelling. Spatial and temporal distributions of atmospheric concentrations of the major air pollutants (main attention was put to NO_2, but we also included O_3, CO, $PM_{2.5}$, SO_2) were considered at the European scale for all public holidays of 2018. Particular attention was paid to the events with the most-pronounced continental- or regional-scale impact: Christmas and New Year, Easter, May Day vacations, and the last days of Ramadan. The simulations were performed with the chemistry transport model SILAM v.5.7. Three model runs were made: the baseline with no treatment of holidays, the run considering holidays as Sundays, and the run forcing 80% reduction of emissions during holidays, for the week-day sensitive sectors. The emission scaling was applied on a country basis. The model predictions were compared with in-situ observations collected by the European Environment Agency. The experiment showed that even conservative treatment of official holidays has a large positive impact on NOx (up to 30% of reduction of the bias inhomogeneity during the holiday days) and improves the CO, $PM_{2.5}$ and O_3 predictions. In many cases, the sensitivity simulations suggested deeper emission reduction than the level of Sundays. An individual consideration of the holiday events in different countries may further improve their representation in the models: specific diurnal pattern of emissions, additional emission due to fireworks, and different driving patterns.

Keywords: holiday emissions of air pollutants, AQ modelling, SILAM model, AQ model sensitivity

1. Introduction

Air quality (AQ) and its temporal and spatial changes are determined by human activities via the release of various air pollutants (Derwent and Hjellbrekke, 2012; Fu et al., 2020; Hassan et al., 2013; Karl et al., 2019; Kukkonen et al., 2020; Lehtomäki et al., 2018; Shi et al., 2019), and modulated by meteorological conditions (Jacob and Winner, 2009; Jhun et al., 2015; Singh et al., 2013; Sofiev et al., 2020).

The ability of atmospheric composition models to follow the temporal variability of air pollution critically depends on representation of temporal emission profiles by inventories used by the models. Arguably the most-difficult task in this context is to reproduce the variations originating from rare irregular events. Changes in the human behavior during non-working days of various type (Beirle et al., 2003; de Foy et al., 2020, 2016; Elansky, 2020; Gour et al., 2013; Hassan et al., 2013; Xu et al., 2017; Zou et al., 2019; Rozbicka and Rozbicki, 2016), including some religious ceremonies (Dasari et al., 2020), cultural practices (Khezri et al., 2015; Nodehi et al., 2018; Ye et al., 2016), celebratory events and festivities (Hoyos et al., 2020; Jiang et al., 2015; Lai and Brimblecombe, 2017; Retama et al., 2019) cause large variations of emissions of air pollutants, which are hard to quantify and generalize. However, the weekend and (some) holiday effects have certain similarities, which might allow drawing an analogy between weekday vs. weekend and holiday vs. non-holiday pollution levels.

Majority of currently available emission inventories are built as gridded yearly or monthly totals for the key primary pollutants (Frost et al., 2013; Granier et al., 2019, 2011), (https://eccad.aeris-data.fr/, access 20.10.2021). Temporal variations at shorter time scales received less attention but their impact on AQ itself and the model's ability to reproduce the observed concentrations have been considered in several studies (Fu et al., 2013; Gioli et al., 2015; Guevara et al., 2017, 2021; Iriti et al., 2020; McGraw et al., 2010). In particular a crucial role of spatial and temporal resolution of emission inventories for the model's skill scores has been demonstrated (Frost et al., 2013; Gioli et al., 2015; Zhao et al., 2015; Zhou et al., 2020).

Many observations-based studies have been focused on effects of weekends and, sometimes, specific holidays, on pollutants concentrations (Chen et al., 2019; Forster and Solomon, 2003). Lonati et al. (2006) examined the weekend effect on particulate matter (PM_{10} and $PM_{2.5}$) emissions from traffic sources in the city of Milan. The research indicated that concentrations of these compounds in the urban area were lower than the levels during the weekdays. Gour et al. (2013) considered differences in pollution levels during weekends and weekdays in Delhi and showed that the patterns follow the working activities of weekends and weekdays. Parra and Franco (2016), pointed out that the concentration of NO_2, NO_X, CO, and $PM_{2.5}$ in working days is higher than that on weekends but the concentration of O_3 in working days is lower than that of the weekend, due to ozone titration. In (2017), Ding et al. reported that during the Chinese New Year the NOx emissions are usually lower by about 10% reflecting the lower business and industrial activities.. In a recent study, Hua et al. (2021) estimated the holiday effect on $PM_{2.5}$ and NO_2 levels in Beijing by a Generalized Additive Model at 34 air quality monitoring stations during the five heating seasons from 2014 to 2019. According to their results, the holiday effect was much stronger than the weekend effects with increasing $PM_{2.5}$ by 2% to 30% but decreasing NO_2 concentrations.

Khalil et al. (2016) analysed hourly measurements of NOx, non-methane hydrocarbons (NMHCs), ozone (O_3), sulphur dioxide (SO_2), $PM_{2.5}$, and PM_{10} collected at the coastal town of Yanbu, Saudi Arabia, during weekends, Eid, Ramadan, and the Hajj periods and demonstrated that the ozone concentrations remained practically the same over these holidays despite the precursor levels were significantly lower. They reported a substantial increase in night-time emissions during Ramadhan due to the shift of human activities to night time.

The fireworks and bonfires during Christmas and New Year of 2013 and 2014 were recognized as the main sources of $PM_{2.5}$ in Mexico city by Retama et al. (2019). Singh et al. (2019) also considered the impact of fireworks on air quality, visibility, and human health and reported significant changes in the pollutants concentrations and a decrease in visibility. Yao et al. (2019) studied air quality trends and fireworks impact in Shanghai during spring festivals from 2013 to 2017. A decreasing trend of $PM_{2.5}$ in this study revealed the positive effect of the firework regulation on air quality.

Recently, various methods based on observed data and models were applied to measure the impact of COVID-19 lockdown on air pollution. These studies investigated the role of transport and industry sectors on pollutants concentrations during the lockdown (Fan et al., 2020; Grivas et al., 2020; Huang et al., 2020; Menut et al., 2020; Sharma et al., 2020; Wang and Su, 2020).

The above works showed that the effects of isolated events, such as public holidays, can be substantial. Yet its analysis at large scales (e.g., a continent and a full year) is missing and a systematic approach to their incorporation into AQ models is yet to be developed.

The goal of the current paper is to address this gap and to make the first step towards incorporation of the public holidays into the regular atmospheric composition and air quality modelling in Europe. We quantified the added value of a comparatively primitive and conservative way of inclusion of official holidays into temporal profiles of emission of air pollutants. Secondly, a sensitivity study was performed demonstrating the extent of the necessary adjustments and potential benefits of a more detailed region-specific analysis of each specific holiday event.

The paper is organised as follows. The next section presents the methodology of the study: information on the European holidays, ways of their incorporation in the emission temporal profiles, the atmospheric composition model SILAM v.5.7 and its setup, as well as the statistical measures quantifying the holiday effect. The Results section presents the outcome of the annual SILAM computations for 2018 and the impact of the holiday information on the model skills. The Discussion section compares the outcome with other studies and demonstrates the sensitivity of the results to the changes in the holiday emission representation.

2. Materials and methods

2.1. European Holidays

We collected a list of official holidays in Europe from the Calendarific global holidays API (https://calendarific.com/api-documentation?v=2, access 20.10.2021) for the full year of 2018. We considered the events marked with “National holiday”, “Local holiday” or “Common local holiday” as holidays (see examples for some European countries in Table 1 - Table 3). Since the Sunday emission scaling was applied country-wise, the "local" or "common local" holidays might sometimes cover wider territories than they should. However, higher level of details was technically not possible to accommodate, and the choice was between missing some local/regional holidays and covering wider areas than needed for some events. Since "religious" and "observance" holidays were not considered we preferred to include the others. The maximum possible error does not exceed 10% because in 2018 National holidays counted to ~800 country-days whereas Common Local and Local were ~60 and ~80, respectively.

The model computations included all holidays in 2018 but, for the sake of brevity, the analysis below will concentrate on the Christmas and New Year weeks, Easter, and May Day (analysed at the European scale), and the Festival of Breaking the Feast at the last days of Ramadan (Eid al-Fitr, analysed for Turkey).

Table 1. Official holidays, example of Finland, 2018.

1 Jan	New Years' Day	10 May	Ascension Day	24 Dec	Christmas Eve
6 Jan	Epiphany	22 Jun	Midsummer Eve	25 Dec	Christmas Day
30 Mar	Good Friday	23 Jun	Midsummer	26 Dec	Boxing Day
2 Apr	Easter Monday	3 Nov	All Saints' Day		
1 May	May Day	6 Dec	Independence Day		

Table 2. Official holidays, example of Germany, 2018.

1 Jan	New Years' Day	10 May	Ascension Day	26 Dec	Boxing Day
30 Mar	Good Friday	21 May	Whit Monday		
2 Apr	Easter Monday	3 Oct	Day of German Unity		
1 May	May Day	25 Dec	Christmas Day		

Table 3. Official holidays, example of Turkey, 2018.

1 Jan	New Year's Day	15 Jul	Democracy and National Unity Day
23 Apr	National Sovereignty and Children's Day	21 Aug	Sacrifice Feast
1 May	Labor and Solidarity Day	22 Aug	Sacrifice Feast Day 2
19 May	Commemoration of Atatürk, Youth and Sports Day	23 Aug	Sacrifice Feast Day 3
15 Jun	Ramadan Feast	24 Aug	Sacrifice Feast Day 4
16 Jun	Ramadan Feast Day 2	30 Aug	Victory Day
17 Jun	Ramadan Feast Day 3	29 Oct	Republic Day

2.2. Atmospheric composition model SILAM

SILAM (System for Integrated modeLling of Atmospheric coMposition, http://silam.fmi.fi/, access: 20.10.2021) is an offline 3D chemical transport model (Sofiev et al., 2015a), also used for emergency decision support (Sofiev et al., 2006) and inverse atmospheric composition problems (Sofiev, 2019; Vira and Sofiev, 2012). The model incorporates Eulerian and Lagrangian dispersion frameworks and a variety of chemical / physical transformation modules covering the troposphere and the stratosphere (Carslaw et al., 1995; Damski et al., 2007; Gery et al., 1989; Kouznetsov and Sofiev, 2012; Sofiev, 2002, 2000; Sofiev et al., 2010; Yarwood et al., 2005). SILAM features a mass-conservative positive-definite advection scheme based on principles laid down by M.Galperin (Galperin et al., 1996). The model can be run with various resolutions and coverages starting from a kilometre scale over a limited area and up to the whole globe (Brasseur et al., 2019; Kouznetsov et al., 2020; Petersen et al., 2019; Sofiev et al., 2020, 2015b; Xian et al., 2019). The vertical structure of the modelling domain consists of stacked layers starting from the surface. The layers can be defined either in z- or hybrid sigma-pressure coordinates. The model can be driven with a variety of numerical weather prediction or climate models.

2.3. Simulation setup

The simulations were performed for the whole year of 2018 for the European domain with the setup following the operational configuration of SILAM in the Copernicus Atmospheric Monitoring Service (CAMS) regional air quality forecasts, as of November 2020 (https://atmosphere.copernicus.eu, access 20.10.2021). The only exception was a twice coarser grid resolution to reduce the computational costs (Table 4).

Table 4. SILAM setup.

Domain and resolution	25W-45E, 30N-72N, 350 × 210 cells of 0.2° × 0.2° size
Vertical structure	10 stacked layers with upper boundaries at 25, 75, 175, 375, 775, 1500, 2700, 4700, 6700 and 8700m above surface
Boundary conditions	First-day operational C-IFS (Integrated Forecasting System of European Centre for Medium-Range Weather Forecasting ECMWF with online-coupled chemistry) forecasts at 0.4° resolution
Meteorological driver	First-day operational IFS forecasts interpolated to 0.2° × 0.2° regular lon-lat grid
Anthropogenic emissions	CAMS_REG_AP v4.2/2017 with GNFR temporal and vertical profiles (https://eccad.aeris-data.fr/, access 20.10.2021)
Natural emissions	SILAM sea-salt (Sofiev et al., 2011), dynamic biogenic emissions based upon Poupkou et al. (2010), mineral dust
Chemical and aerosol transformations	Modified CBM-5 gas-phase transformation, SO_4, NO_3, NH_4 ion chemistry, SO_2 oxidation, nitrate formation, Volatility-basis set for secondary organics

Deposition	Dry: Resistance approach (Wesely, 1989) for gases, (Kouznetsov and Sofiev, 2012) for aerosols, Wet: SILAM v2018 wet deposition scheme

The anthropogenic emissions in CAMS_REG_AP v4.2 inventory were used as maps of annual totals separately for each country and 16 GNFR sectors (Gridded Nomenclature For Reporting, European Environment Agency., 2013). To obtain the hourly emissions, the annual means were scaled with three temporal profiles, defined separately for each sector, corresponding to month-of-year (MOY), day-of-week (DOW), and hour-of-day (HOD) (Granier et al., 2019). In the CAMS-regional operational setup, the anthropogenic emissions are used without accounting for public holidays.

To assess the sensitivity of pollutant concentrations during holidays, three SILAM runs were made: the baseline with no special holiday treatment (hereinafter, the BL case), with the holiday days considered as Sundays (the HS case), a sensitivity-test run with 80% of emission reduction during holidays (the R3). The emission scaling for HS and R3 cases were applied only to the sectors affected by the DOW profile. The R3 case was constructed for the Discussion section as a definite low boundary of the possible holiday effect with no realistic scenario behind. Technically, the emissions were adjusted by altering the DOW scaling coefficients for dates and countries where the holidays occur. For the HS case the coefficients were set to their Sunday values, and for the R3 case they were forced to 0.2. The DOW coefficients for the affected sectors are shown in Figure 1. Other sectors (D_Fugitives, G_Shipping, H_Aviation, I_OffRoad, J_Waste, K_AgriculturalLivestock, and L_AgriculturalOther) have unity DOW coefficients for all three cases.

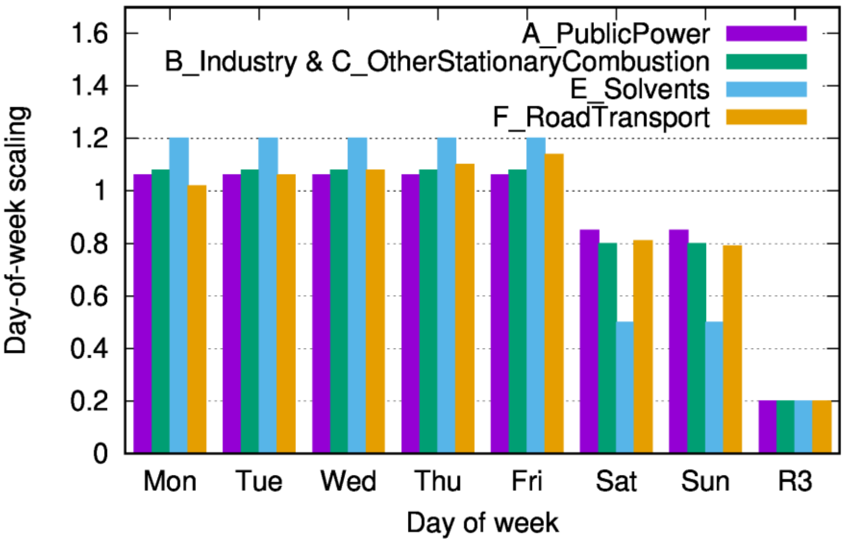

Figure 1. Day-of-week coefficients for the affected sectors. R3 is the value forced for national holidays for the R3 case.

3. Evaluation scores

For evaluation of the simulations, we used the hourly data of the AQ monitoring stations downloaded from the European Environmental Agency portal (EEA, http://discomap.eea.europa.eu/map/fme/AirQualityExport.htm, access 20.10.2021). Since we focus on regional-scale effects, a subset of representative stations was selected, namely, the stations classified from 1 to 7 according to Joly and Peuch (2012) classification. This dataset is also used for the operational CAMS-regional evaluation (751 stations over the European domain). For the Ramadan analysis, only Turkish stations were used, with no classification-related filtering applied to maintain sufficient number of stations in the analysis.

The effect of holidays was considered for the main pollutants observed by the EEA network: $PM_{2.5}$, SO_2, CO, NO_2, NO_x, and O_3. Five statistics were considered following the CAMS evaluation standards: bias, fractional bias (FracB), Pearson correlation coefficient (corr), RMSE, and fractional gross error (FGerr). We considered the effect of holidays at two temporal scales. The short-term impact was analysed for the one-to-two weeks-long period centred around each holiday day. For each day of this period, the spatial statistics were computed across the observational stations, and evolution of these statistics from day to day was compared between the SILAM runs. The long-term longitudinal effect was analysed at annual level for the whole 2018 and attention was given to the temporal statistics computed for the stations time series.

Since the diurnal profile of emission during holidays is unknown and probably specific for each event and country, the current study mainly used daily averaging of both observational and model data for computations of the statistics.

Assessing the effect of holidays on the model skills is not straightforward because the emission error during holidays (e.g., too high NOx emission) can offset the general under-estimation of the emission in the region, as well as the model internal uncertainties. As a result, the model results without the holiday effect may be even better than with it – but for wrong reason. To avoid this problem, we considered the variability of the time series of the model skills as the main measure of success. For instance, correctly represented holiday effect would lead to the same model bias during the holiday day as before and after. A quantitative measure of success is therefore the ratio *R* of standard deviations of the HS and BL runs:

(1) $$R\_P = \frac{stdev(P_{HS})}{stdev(P_{BL})},$$

where *P* is one of the above CAMS spatial model skills and standard deviation is taken among the daily values of this skill. The positive effect of the holiday emission scaling would mean $R < 1$, whereas $R > 1$ indicated that the actual emission moved into opposite direction than suggested by the Sunday scaling coefficients.

4. Results

4.1. Overall short-term impact of public holidays

The summary of the simulations is presented in Figure 2 for the main holidays of 2018 and all considered pollutants. The physical meaning of the *R*-criterion (1) is illustrated in Figure 3, which shows a substantial "jump" in all model skills at or around the Christmas day. Before and after that day the skill values are similar. The HS run exhibits less of a jump than the BL case, which indicates that the model-measurement agreement is more homogeneous. The ratio of the standard deviations of the skills *R* from Eq. (1) is presented in Figure 2 for all skills and all species.

The effect, expectedly, varies between the quality metrics and species. Thus, the least sensitive parameter is RMSE whereas the spatial correlation coefficient showed mixed signals in loose connection with other parameters. The most-sensitive parameters are bias, fractional bias and fractional gross error, which are also the most-important for the study.

The majority of metrics and cases showed clear positive effect of accommodating the holiday emission changes in the model simulations. The most-significant changes were obtained for NO_2 and NOx, where the flattening of, e.g., fractional bias time series could be as large as 10-20%. It reflects the major role of the changes in the traffic intensity (mostly, reduction) during holidays. Carbon monoxide generally followed the NOx patterns but with a lower effect due to a large background level and the contribution from the sources with weak or no weekly variation of the intensity. Changes of O_3 and SO_2 were very limited, except for Christmas when they also showed more homogeneous bias of the HS run.

Intriguingly, the effect for $PM_{2.5}$ and PM_{10} was significant for fractional bias and fractional gross error (but small for bias) and partly detrimental. It indicates that the Sunday profiles for primary PM and, possibly, NH_3 emission may be not suitable for holidays. Domestic activities, seemingly adding little to NOx emissions, may be quite significant for emission of PM and PM precursors. It was particularly evident for May Day, which is usually characterised by intense outdoor activities all over Europe.

Holiday-wise, the most-significant impact was obtained for Christmas while Easter and Ramadan (assessed for Turkish stations only) showed moderate improvement. The May Day showed mixed signal mentioned above.

(Std HS/Std BL)							
Mayday (Europe), (13 days, 29th Apr- 12th May)							
	O_3	NO_2	PM_{10}	$PM_{2.5}$	SO_2	CO	NO_X
R_RMSE	1.00	1.00	1.00	1.00	1.00	0.98	1.00
R_corr	1.05	0.97	1.02	0.97	1.00	1.04	0.97
R_bias	1.00	0.96	1.02	1.00	1.00	0.97	0.99
R_FracB	1.02	0.82	1.09	1.12	1.26	1.01	0.86
R_FGerr	1.01	0.86	1.13	1.11	1.22	0.97	0.88
Christmas (Europe), (12 days, 19th Dec-31th Dec)							
R_RMSE	1.00	1.00	1.00	1.00	1.00	0.99	0.98
R_corr	1.01	0.92	1.00	0.99	1.00	1.01	1.04
R_bias	0.95	0.97	0.99	1.00	1.00	0.94	0.93
R_FracB	0.84	0.87	0.93	0.89	0.87	0.84	0.86
R_FGerr	1.00	0.97	0.84	0.91	0.97	0.85	0.93
Easter (Europe), (9 days, 28th Mar-6th Apr)							
R_RMSE	1.00	1.00	1.00	1.00	1.00	0.97	0.99
R_corr	1.01	0.95	1.00	1.03	1.02	1.03	1.01
R_bias	0.99	0.98	0.99	1.00	1.00	0.97	0.97
R_FracB	0.98	0.87	0.97	0.95	1.00	0.96	0.89
R_FGerr	1.04	0.88	1.02	1.02	1.01	1.05	0.89
Ramadan (Turkey), (33 days, 16^{th} June- 18^{th} July)							
R_RMSE	1.00	1.00	1.00	1.00	1.00	0.97	0.99
R_corr	1.01	0.95	1.00	1.03	1.02	1.03	1.01
R_bias	0.99	0.98	0.99	1.00	1.00	0.97	0.97
R_FracB	0.98	0.87	0.97	0.95	1.00	0.96	0.89
R_FGerr	1.04	0.88	1.02	1.02	1.01	1.05	0.89

Figure 2. Summary of the *R* value for the main European holidays in 2018 for the considered air pollutants (the effect of Ramadan is assessed for Turkey only).

4.2. Examples of specific holidays

The impact of holidays on the SILAM spatial skills was the largest for the Christmas week (Figure 2 and Figure 3). As expected, the Christmas period is characterised by lower emissions, which resulted in a high bias of the BL model run and almost 50% growth of the RMSE compared to the surrounding days. The reduction of emission in the HS run improved the performance but did not eliminate the problem: the time series of the skills still exhibit strong jumps on (and around) the Christmas day. Comparison of daily-mean concentrations showed reduction of the model bias for the HS run by ~4.5 µg m^{-3} of NO_2. Consequently, the RMSE was also lower, by ~4 µg m^{-3}. These improvements constitute about 26% of the baseline statistics (see Figs. S1-S6 in the Supplementary section for other species). However, as seen from the bias time series (Figure 3), the HS run, being a step in the right direction, incorporated only a small fraction of the actual emission reduction, which also started before and ended after the Christmas day.

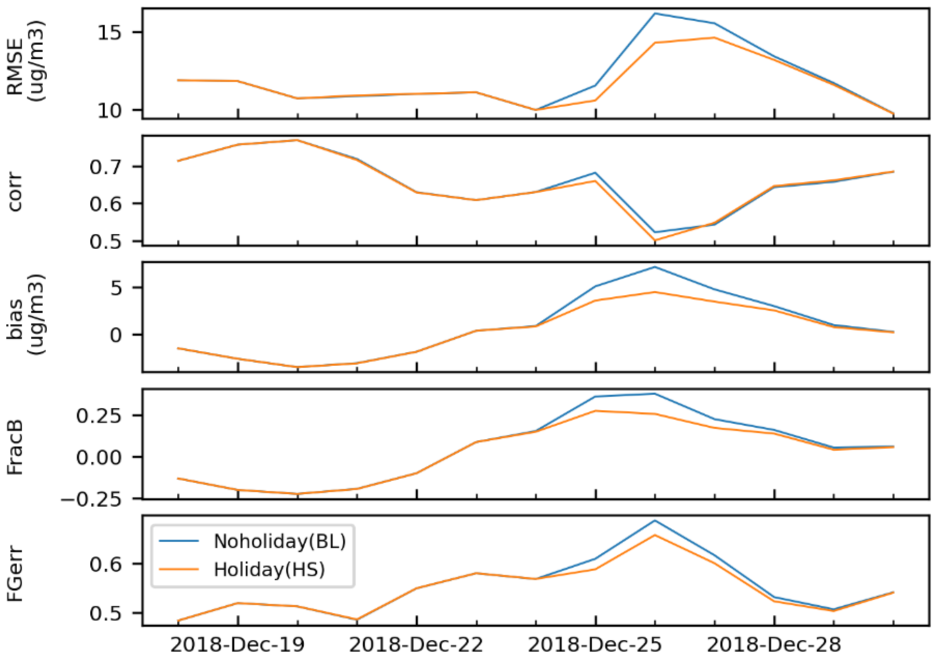

Figure 3. SILAM daily-mean spatial scores for Christmas (NO_2, whole Europe).

Comparing the HS and BL runs for Easter (Figure 4), one can see a substantial improvement of the scores for the days of the event. Similarly to the winter holiday week, Easter emission reduction seems to be deeper than that of Sundays but the difference is not so large (see results for other species in the Supplementary Materials, Figs. S7- S12).

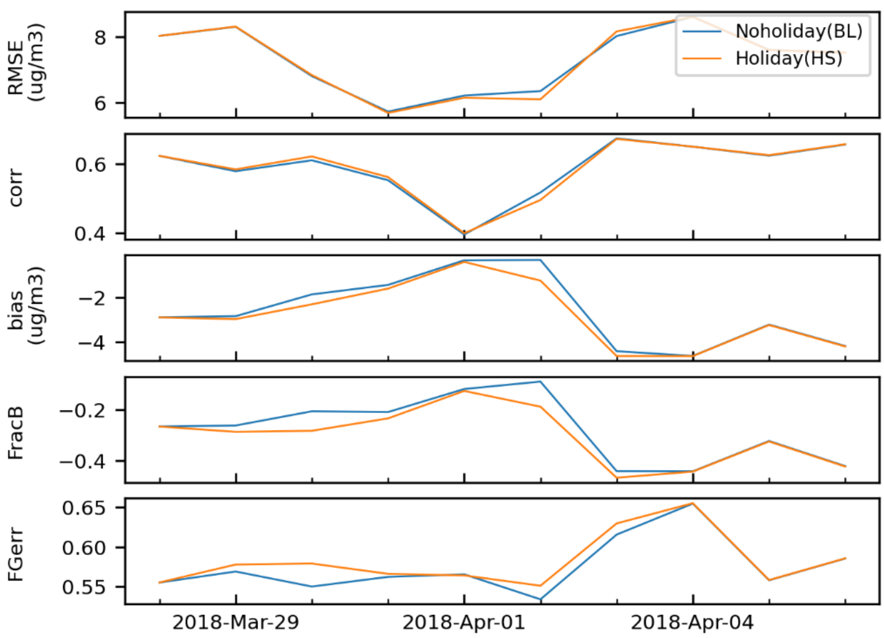

Figure 4. SILAM daily-mean spatial scores for Easter (NO_2, whole Europe).

The first 10 days of May were considered as an example of late-spring / summer vacations (there are no whole-Europe holidays during summer itself). The HS run showed slightly lower values for RMSE but, similarly to Easter, initially negative bias increased further. Nevertheless, the bias time series became smoother comparing to the BL one, which is an indication of the improvement: the systematic emission under-estimation is a separate task, which necessity should not be masked by another error. Reduction of NOx resulted in a substantial improvement of the ozone scores (Supplementary Material, Figs. S13- S18). This connection was the strongest among all holidays throughout the year, owing to the active chemistry and photolysis in May.

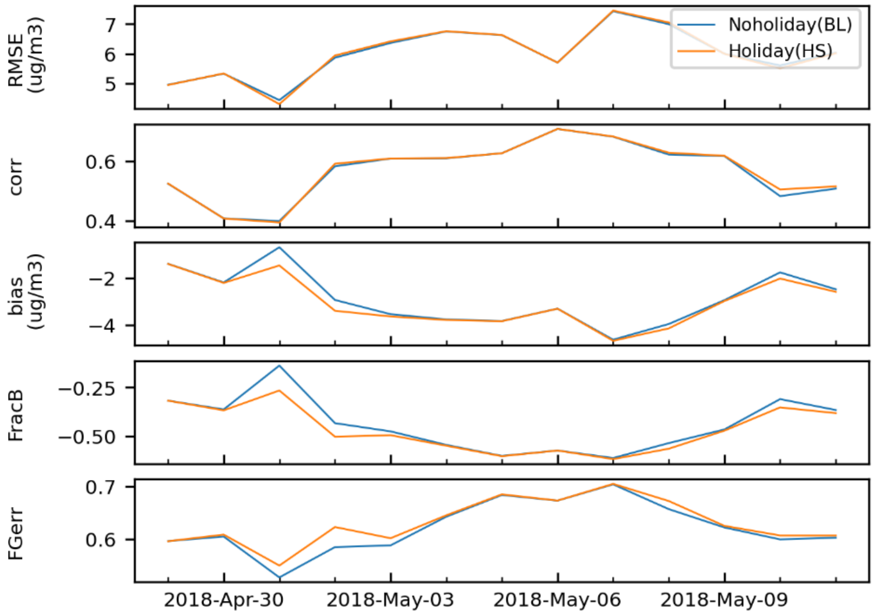

Figure 5**.** SILAM daily-mean spatial scores for May vacations (NO_2, whole Europe).

In the Muslim countries (Turkey, Albania), the Ramadan month is not a public holiday, only working hours are reduced, which is not reflected in the HS run. Only the last three days of Ramadan - the Ramadan Feast – are the public holidays in Turkey (Table 3, Figure 2, Figure 6 for NO_2, Supplementary material for other species, Figs. S19- S24). For these days, there are distinct differences between the BL and HS model runs. However, similarly to Easter and the May Day, the model is generally low biased for NO_2 in Turkey during this period, therefore the additional reduction of the concentrations is, formally speaking, not an improvement: the negative bias increases. Nevertheless, it is a step in the right direction, as seen from the reduced variations of the model skills of the HS run (Figure 2). Due to this under-estimation, it is difficult to say how conservative the Sunday-level emission reduction is for these holidays (Figure 6). Unlike the Christmas and Easter holidays, which exist in most European countries, the Ramadan Feast days substantially affect only Turkish stations. At the European scale, the effect is negligible.

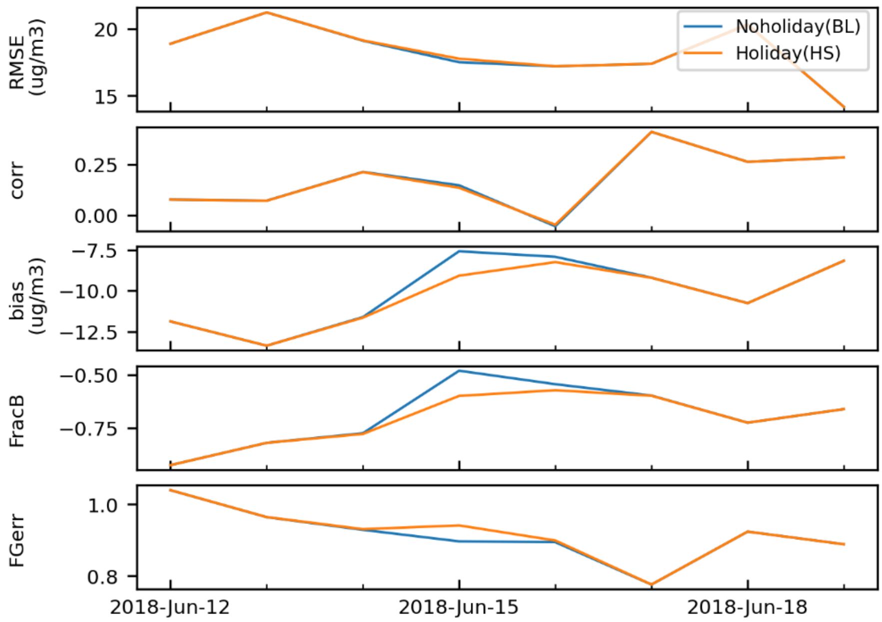

Figure 6**.** SILAM daily-mean spatial scores for Ramadan (NO_2, only stations in Turkey).

4.3. Long-term statistics

At the annual scale, the impact of holidays on the model performance is limited. The reduction affects only the days with changed emissions and practically does not influence already the next day. The most-significant impact was for Christmas and New Year weeks but even for them the effect faded out by the next day. According to the annual statistics, at annual level the overall effect for NO_2 for the whole Europe was positive but did not exceed 1%, which reflects the typical number of holiday days in a year (< 3%) and up to ~30% improvement during these days. Impact on other species was lower than that for NO_2.

5. Discussion

5.1. Impact of holiday effect on model skills: episodically significant, noticeable at annual level

The simulations presented in the previous section confirmed that the official holidays substantially affect air quality, as also shown in the studies outlined in the Introduction. The holiday incorporation into the simulations as Sundays, being very simple technically, brings noticeable improvement of the model skills for the days with the modified emission. Since the number of such days in each year is < 3%, the overall improvement of the annual skills is within 1%, which is quite significant at such level of aggregation.

The suggested simple approach should be considered as only the first step. Holidays are characterised by redistribution of emission due to changing traffic structure, shift of activities from office areas to suburbs, etc. Incorporation of these effects can further improve the model skills but will require quantitative information on such redistribution at the European level. Several approaches towards determining these profiles have been reported, e.g. (Guevara et al., 2021; Mues et al., 2014; Menut et al., 2012), but tests with SILAM showed no substantial improvement suggesting additional uncertainties in the proposed profiles. Some support can be found from traffic information, which is presently not available at continental scales (examples for two cities are provided below).

5.2. Sunday-based emission reduction for holidays is a conservative estimate

The simulations also suggested a comparatively simple way to achieve a more significant gain: the Sunday emission scaling (Figure 1) can be amplified. In a few cases, especially for the Christmas and New Year, the actual emission rates might be much lower, whereas for some events the emission of some species might increase. Thus, the New Year night celebration in many countries involves fireworks, which add substantial amount of PM. The second issue is that the Sunday diurnal profile of traffic (also other sources) is substantially different from that of the weekdays. In the present version of SILAM this difference is not accounted for, which evidently limits the model performance and the gain due to the holiday incorporation.

This is consistent with the estimates of the observations-based studies. Thus, Hua et al (2021) also found that the holiday effect is much stronger than the weekend effects. They noticed the opposite signs for $PM_{2.5}$ and NO_2: average increase of about 22% and average decrease of about 11%, respectively. Similarly, Retama et al., (2019) reported a substantial effect of fireworks on PM at night and the following morning of Christmas Day and the New Year's day. Along the same lines, Rozbicka and Rozbicki (2016), demonstrated that daily mean ozone concentration and maximum ozone peaks are respectively 13% and 8% higher than those on the weekdays, which also indicates a reduction in NO2 concentrations of about 20%. Conversely, Nodehi et al. (2018) study showed that the Norooz holidays (the Iranian New Year, or a spring festival), are characterised by a reduction of concentration of $PM_{2.5}$ due to the reduction of the working activities and no massive fireworks. The reported reduction of $PM_{2.5}$ concentration during the Ramadan Feast holidays is quite close to our estimates.

5.3. Regional specifics of the effect of HS and R3 emission reduction

The impact of holidays-related emission reduction varies from country to country with substantial differences visible even at a sub-country level. To highlight these peculiarities, we used the station-wise temporal correlation coefficients for hourly NO_2, CO, O_3, and $PM_{2.5}$ concentrations (Figure 7, - Figure 9). The maps reveal a strong inhomogeneity of the effect for Christmas and New Year weeks (Figure 7), as well as for May Day (Figure 8). It can dramatically vary even within a single country – as seen from the comparison of maps of Figure 7 and country-median correlation coefficient of Figure 9.

In the case of NO_2, correlation increases, e.g., in Northern Germany, Italy, Poland and Eastern part of Finland for both HS and R3 runs: reduction of emission had led to lower concentrations, which improved temporal correlation for these regions. Conversely, there was no effect or even deterioration of correlation in Southern Germany, Northern France, Madrid region, etc.

Other species showed qualitatively similar patterns but lower gains and losses. Significant changes are noticeable only for CO, which is also significantly affected by traffic. Minor changes for ozone were noticeable only in winter when NOx emissions affect O_3 concentrations via titration. This is consistent with the spatial statistics of Figure 2. For PM, the effect was not unequivocal: there is a small but coherent reduction of correlation in Eastern Europe in May but neutral response or an increase for Christmas. This once again refers to the regional habits of celebration of these holidays and corroborates with the overall detrimental effect on these species reported in Figure 2. One should also keep in mind that the fireworks are used during the New Year celebration only in some countries (as suggested by the current results, Western Europe), where the HS and R3 runs are clearly inadequate for PM.

Surprisingly, for the Christmas holidays, skills over most of France are generally worse for the HS run and much worse for R3 indicating a substantially different pattern of activities during holidays, compared to those of the neighboring countries: reduction of NOx emissions and, consequently, concentrations there does not correlate with he observed tendencies. For May Day, the specificity did not show up: correlation has noticeably increased over most of the country, similar to its neighbors. Among the hypothetical reasons for such behavior, one could suggest more “active” habits for Christmas celebration in France than in the neighboring countries.

The R3 run, which was planned as an overshot, showed strong improvement of temporal correlation over Christmas week in Eastern Europe, Central and Northern Italy and Northern Germany. Therefore, one can argue that even the 5-fold emission reduction in these countries / regions might be not that much of an exaggeration.

These issues deserve a more detailed analysis accounting for the varying traffic patterns and effects on days preceding to and following the official holidays.

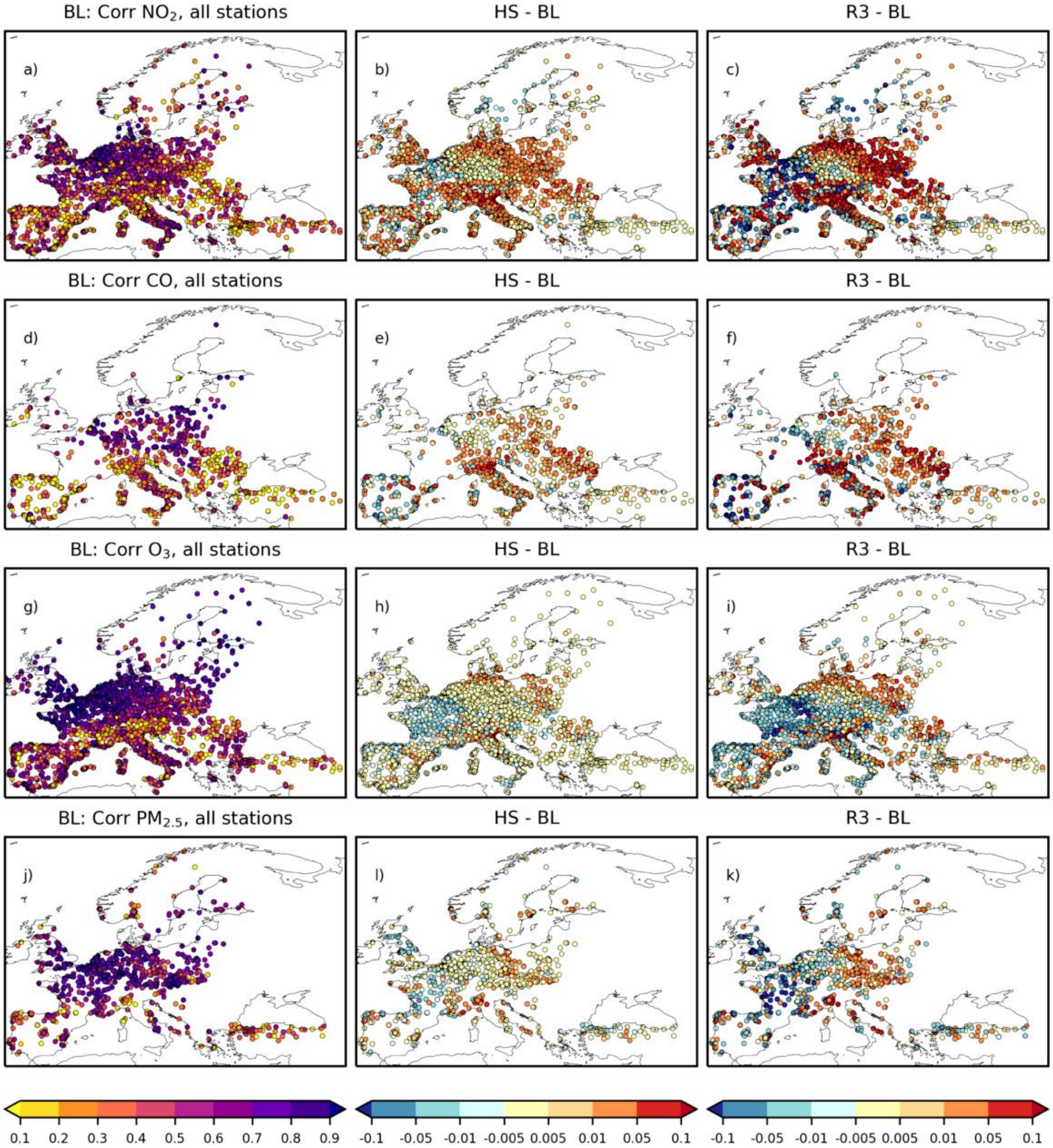

Figure 7**.** Maps of the temporal correlation coefficient of hourly NO_2, CO, O_3, and $PM_{2.5}$ concentrations for the EEA stations during the Christmas holidays (21-31 December 2018).

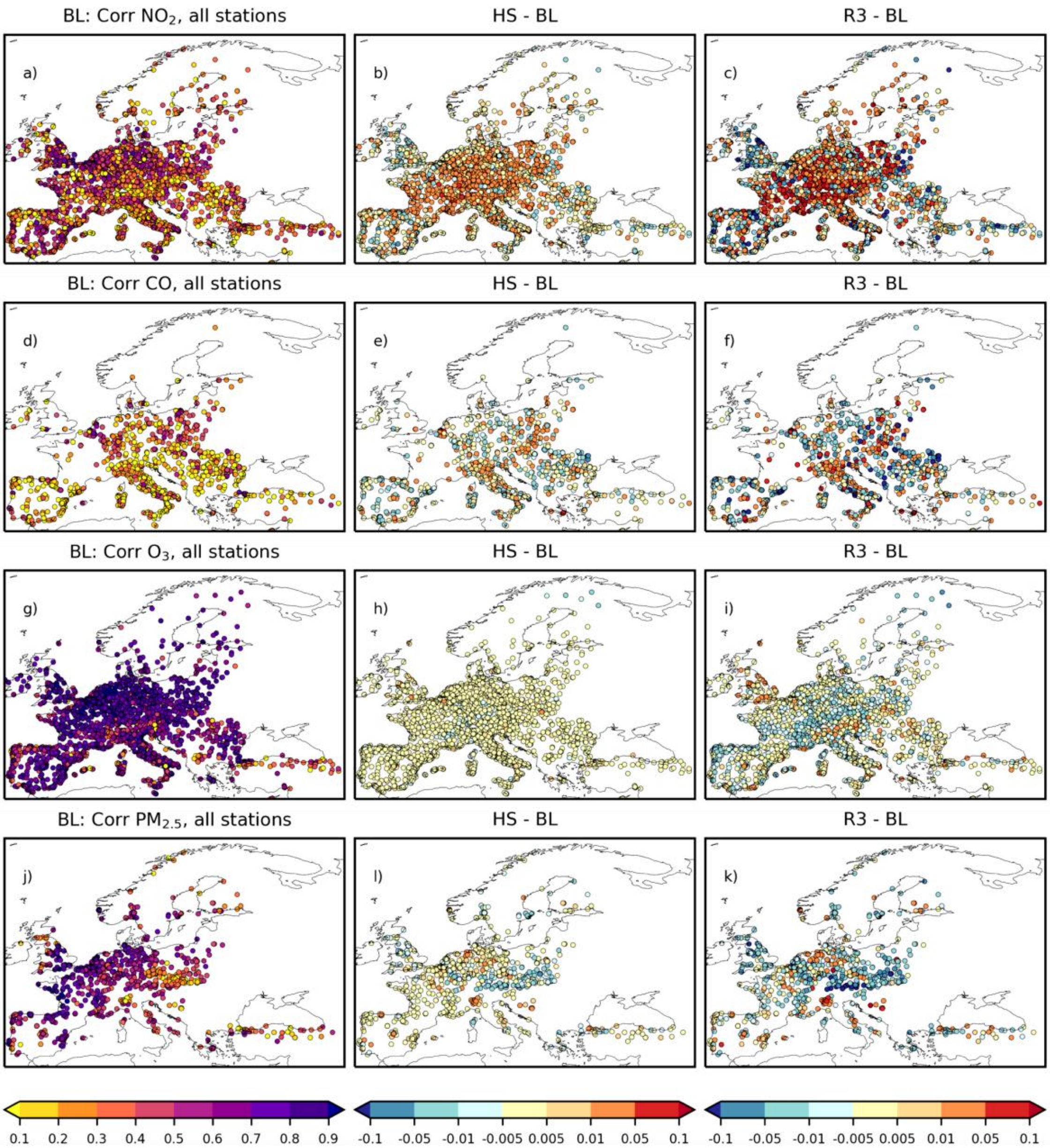

Figure 8. Maps of the temporal correlation coefficient of hourly NO_2, CO, O_3, and $PM_{2.5}$ concentrations for the EEA stations during the May Day holidays (29 April – 11 May 2018).

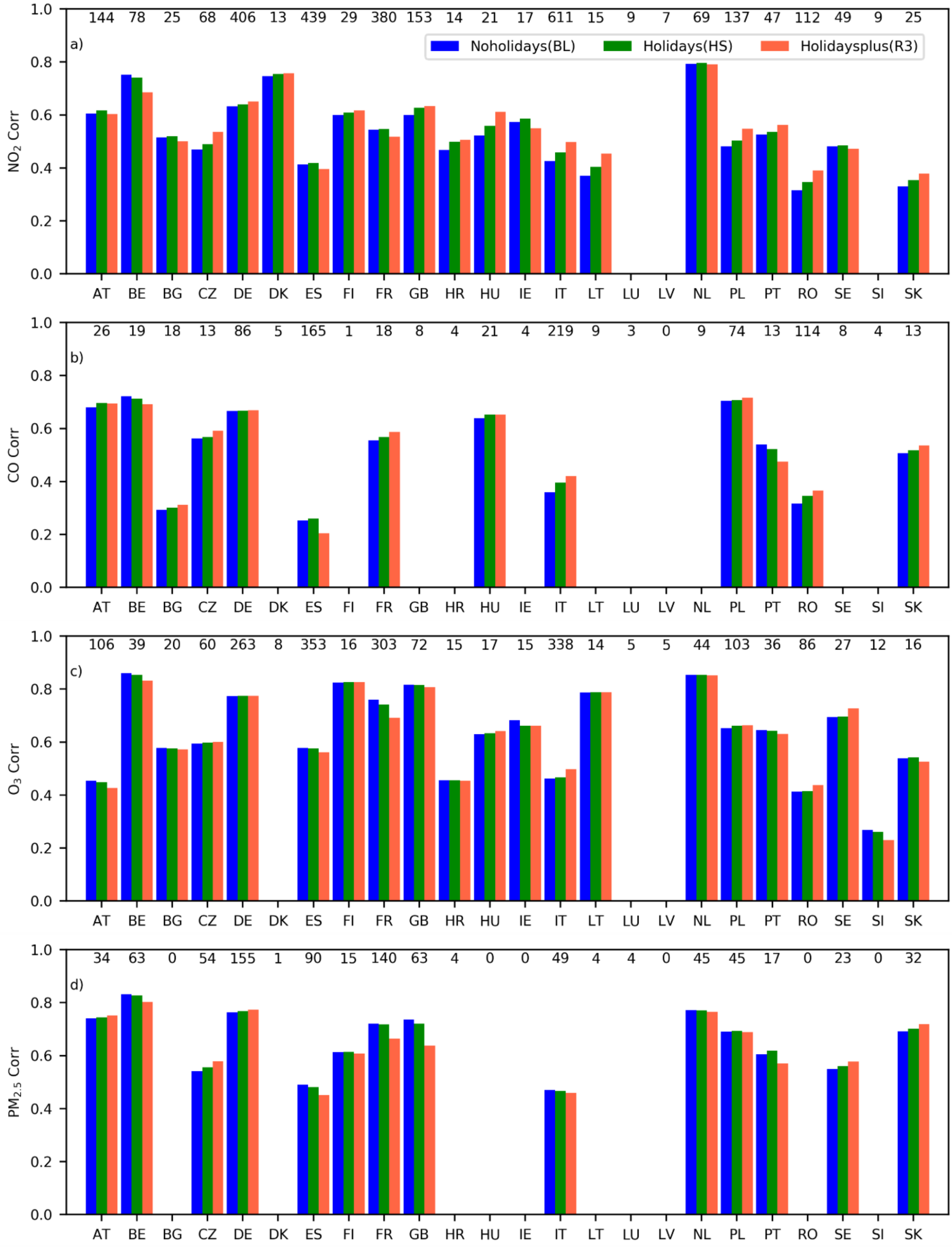

Figure 9. Country-wise median change of temporal correlation coefficient during two weeks of Christmas holidays (21-31 December 2018). The numbers at the top of each panel show the number of stations that reported data for the period.

5.4. Local traffic counts illustrate the phenomenon

As mentioned above, a lack of systematic continental-scale traffic counts precludes their usage for determining and/or verifying the assumptions of the current study. However, for a few cities the data are available and can be used as illustration of the effect. Below we provide the time series for Helsinki and Dublin (Figure 10). The daily traffic counts over several years corroborate / illustrate the above discussion. Indeed, for Helsinki, the May Day traffic count almost perfectly meets the Sunday number of cars 3 days before in 2019 and one day after in 2020. The difference between the years illustrates the COVID-19 lockdown effects in 2020.

For Dublin, Christmas – New Year holidays for two sequential years show that for this major event the traffic reduction is at least two times deeper than for ordinary Sunday: almost 4 times less cars were counted on 25-26 December than in ordinary day. Such reduction is already comparable with the 5-fold reduction of the S3 run. The city also manifests about-twice lower traffic intensity during COVID-19 lockdowns whereas Helsinki lost about 30% of its traffic. Finally, one can see that the traffic does not restore to normal intensity between Christmas and New Year, similar to what was noticed from the observations Figure 3.

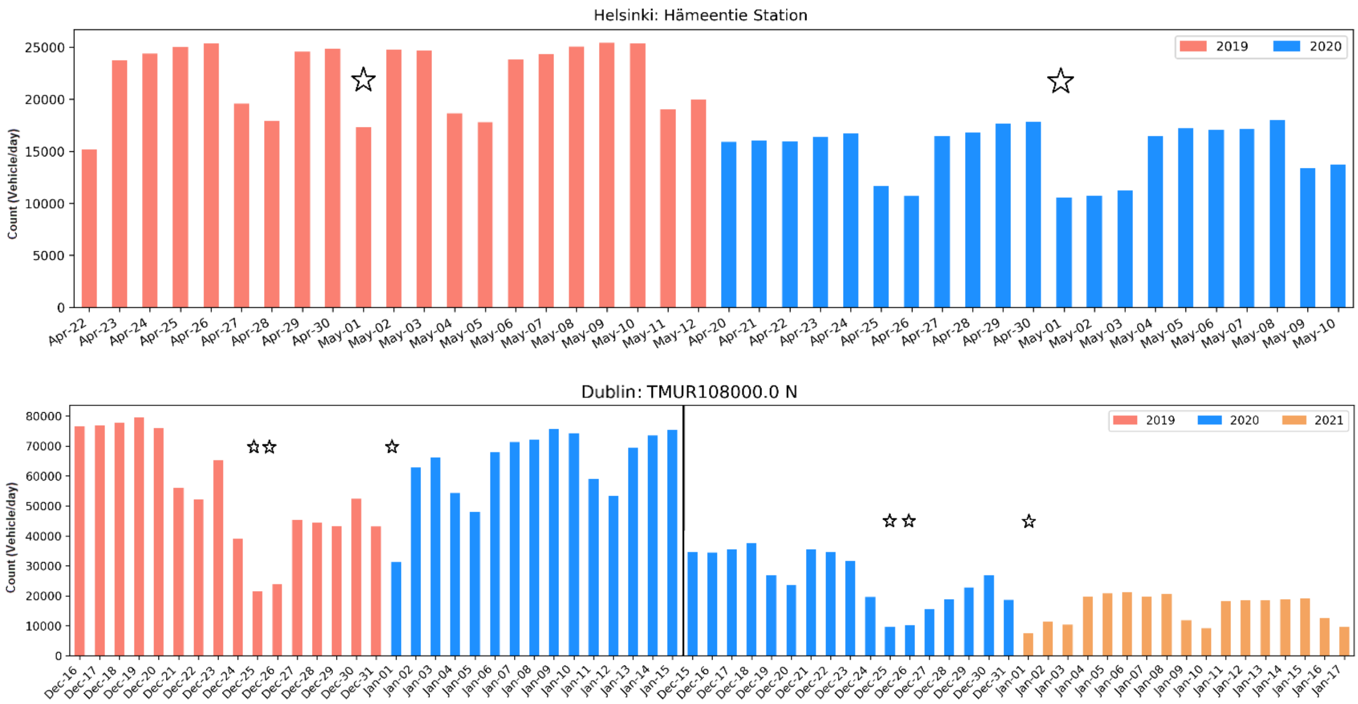

Figure 10. Daily traffic count in Helsinki (upper panel) and Dublin (lower panel) during Christmas / New Year and May Day holidays. Stars mark the official holidays. Obs non-holiday day of 6 January in Dublin.

6. Summary

Incorporation of information on public holidays in emission of the affected anthropogenic sectors leads to substantial short-term improvements of the SILAM model scores, even if done conservatively. The largest impact was found for NOx, which is controlled by the changes of the traffic intensity. Certain improvements were also found for other species but the signal was weaker than that for NOx.

The effect of the emission reduction during holidays may look detrimental in case of a systematic under-estimation in some regions. However, in majority of such cases the bias and other skills became more homogeneous in time manifesting reduction of the holiday-induced errors in emission.

The sensitivity runs confirmed that the Sunday emission level, in many cases, is a too conservative proxy for the public-holiday emission. Thus, the reduction during Christmas and New Year holidays of 2018 was closer to a factor of 4 in Western Europe and possibly even stronger in Eastern Europe.

The current experiment used the prescribed sector-specific diurnal profiles of emission intensity, same for weekdays, weekends, and holidays. Incorporation of specific profiles for weekends and holidays, might further improve the quality of the model predictions.

The proposed method of handling emission reduction in AQ models, albeit very simple and with a room for improvement, gives noticeable gains in the model performance. The method is straightforward to implement in the AQ models and can be considered as an easy way to improve the model prediction skills for the periods of public holidays. An in-depth analysis of the specific holidays and related traditions in specific countries, such as fireworks in New Year night, would, most probably, lead to further improvements of the AQ predictions.

7. Code and data availability

SILAM is an open-code system and can be obtained from the GitHub open repository https://github.com/fmidev/silam-model. The simulation results are available on request from the authors of the paper.

8. Author contribution

The authors jointly devised the project and developed the paper concept. YF contributed to the implementation of the research and analysis of the results and drafted the paper. RK performed the SILAM computations and contributed to the analysis. MS contributed to the analysis, drafted the Discussion and contributed to other sections of the paper. All authors edited the final text.

9. Acknowledgements

The study was performed within the scope of Academy of Finland project GLORIA (grant Nbr 310372). Financial support of Copernicus Atmospheric Monitoring Service (CAMS-50 and CAMS-61) for the SILAM development is kindly acknowledged.

10.References

Beirle, S., Platt, U., Wenig, M., and Wagner, T.: Weekly cycle of NO2 by GOME measurements: a signature of anthropogenic sources, 8, 2003.

Brasseur, G. P., Xie, Y., Petersen, A. K., Bouarar, I., Flemming, J., Gauss, M., Jiang, F., Kouznetsov, R., Kranenburg, R., Mijling, B., Peuch, V.-H., Pommier, M., Segers, A., Sofiev, M., Timmermans, R., van der A, R., Walters, S., Xu, J., and Zhou, G.: Ensemble forecasts of air quality in eastern China – Part 1: Model description and implementation of the MarcoPolo–Panda prediction system, version 1, 12, 33–67, https://doi.org/10.5194/gmd-12-33-2019, 2019.

Carslaw, K. S., Luo, B., and Peter, T.: An analytic expression for the composition of aqueous HNO_3 -H_2SO_4 stratospheric aerosols including gas phase removal of HNO_3, Geophys. Res. Lett., 22, 1877–1880, https://doi.org/10.1029/95GL01668, 1995.

Chen, P.-Y., Tan, P.-H., Chou, C. C.-K., Lin, Y.-S., Chen, W.-N., and Shiu, C.-J.: Impacts of holiday characteristics and number of vacation days on “holiday effect” in Taipei: Implications on ozone control strategies, Atmospheric Environment, 202, 357–369, https://doi.org/10.1016/j.atmosenv.2019.01.029, 2019.

Damski, J., Thölix, L., Backman, L., Taalas, P., and Kulmala, M.: FinROSE — middle atmospheric chemistry transport model, 12, 535–550, 2007.

Dasari, H. P., Desamsetti, S., Langodan, S., Karumuri, R. K., Singh, S., and Hoteit, I.: Atmospheric conditions and air quality assessment over NEOM, kingdom of Saudi Arabia, Atmospheric Environment, 230, 117489, https://doi.org/10.1016/j.atmosenv.2020.117489, 2020.

Derwent, R. and Hjellbrekke, A.-Gunn.: Air Pollution by Ozone Across Europe: Handbook of Environmental Chemistry, Springer, Berlin, Heidelberg, 371 pp., 2012.

Ding, J., Miyazaki, K., Cho, S., Janssens-Maenhout, G., Zhang, Q., Liu, F., and Levelt, P. F.: Intercomparison of NOx emission inventories over East Asia, 17, 2017.

Elansky, N. F.: Weekly patterns and weekend effects of air pollution in the Moscow megacity, 15, 2020.

European Environment Agency.: EMEP/EEA air pollutant emission inventory guidebook 2013: technical guidance to prepare national emission inventories., Publications Office, LU, 2013.

Fan, C., Li, Z., Li, Y., Dong, J., van der A, R., and de Leeuw, G.: Does reduction of emissions imply improved air quality?, Gases/Remote Sensing/Troposphere/Chemistry (chemical composition and reactions), https://doi.org/10.5194/acp-2020-1101, 2020.

Forster, P. M. de F. and Solomon, S.: Observations of a “Weekend Effect” in Diurnal Temperature Range, 100, 11225–11230, 2003.

de Foy, B., Lu, Z., and Streets, D. G.: Impacts of control strategies, the Great Recession and weekday variations on NO 2 columns above North American cities, Atmospheric Environment, 138, 74–86, https://doi.org/10.1016/j.atmosenv.2016.04.038, 2016.

de Foy, B., Brune, W. H., and Schauer, J. J.: Changes in ozone photochemical regime in Fresno, California from 1994 to 2018 deduced from changes in the weekend effect, Environmental Pollution, 263, 114380, https://doi.org/10.1016/j.envpol.2020.114380, 2020.

Frost, G. J., Middleton, P., Tarrasón, L., Granier, C., Guenther, A., Cardenas, B., Denier van der Gon, H., Janssens-Maenhout, G., Kaiser, J. W., Keating, T., Klimont, Z., Lamarque, J.-F., Liousse, C., Nickovic, S., Ohara, T., Schultz, M. G., Skiba, U., van Aardenne, J., and Wang, Y.: New Directions: GEIA’s 2020 vision for better air emissions information, Atmospheric Environment, 81, 710–712, https://doi.org/10.1016/j.atmosenv.2013.08.063, 2013.

Fu, D., Song, Z., Zhang, X., Wu, Y., Duan, M., Pu, W., Ma, Z., Quan, W., Zhou, H., Che, H., and Xia, X.: Similarities and Differences in the Temporal Variability of PM2.5 and AOD Between Urban and Rural Stations in Beijing, Remote Sensing, 12, 1193, https://doi.org/10.3390/rs12071193, 2020.

Fu, X., Wang, S., Zhao, B., Xing, J., Cheng, Z., Liu, H., and Hao, J.: Emission inventory of primary pollutants and chemical speciation in 2010 for the Yangtze River Delta region, China, Atmospheric Environment, 70, 39–50, https://doi.org/10.1016/j.atmosenv.2012.12.034, 2013.

Galperin, M. V., Maslyaev, A. M., Pekar, M. I., and Sofiev, M.: The development of HM model in 1996, Meteorological Synthesising Centre East, Moscow, 1996.

Gery, M. W., Whitten, G. Z., Killus, J. P., and Dodge, M. C.: A photochemical kinetics mechanism for urban and regional scale computer modelling, 94, 12925–12956, https://doi.org/0148-0227/89/89JD-00793$05.00, 1989.

Gioli, B., Gualtieri, G., Busillo, C., Calastrini, F., Zaldei, A., and Toscano, P.: Improving high resolution emission inventories with local proxies and urban eddy covariance flux measurements, Atmospheric Environment, 115, 246–256, https://doi.org/10.1016/j.atmosenv.2015.05.068, 2015.

Gour, A. A., Singh, S. K., Tyagi, S. K., and Mandal, A.: Weekday/weekend differences in air quality parameters in delhi, india, 1, 69–76, 2013.

Granier, C., Bessagnet, B., Bond, T., D'Angiola, A., Denier van der Gon, H., Frost, G. J., Heil, A., Kaiser, J. W., Kinne, S., Klimont, Z., Kloster, S., Lamarque, J.-F., Liousse, C., Masui, T., Meleux, F., Mieville, A., Ohara, T., Raut, J.-C., Riahi, K., Schultz, M. G., Smith, S. J., Thompson, A., van Aardenne, J., van der Werf, G. R., and van Vuuren, D. P.: Evolution of anthropogenic and biomass burning emissions of air pollutants at global and regional scales during the 1980–2010 period, Climatic Change, 109, 163–190, https://doi.org/10.1007/s10584-011-0154-1, 2011.

Granier, C., Darras, S., Denier van der Gon, H., Doubalova, J., Elguindi, N., Galle, B., Gauss, M., Guevara, M., Jalkanen, J.-P., Kuenen, J., Liousse, C., Quack, B., Simpson, D., and Sindelarova, K.: The Copernicus Atmosphere Monitoring Service global and regional emissions (April 2019 version), https://doi.org/10.24380/D0BN-KX16, 2019.

Grivas, G., Athanasopoulou, E., Kakouri, A., Bailey, J., Liakakou, E., Stavroulas, I., Kalkavouras, P., Bougiatioti, A., Kaskaoutis, D. G., Ramonet, M., Mihalopoulos, N., and Gerasopoulos, E.: Integrating In Situ Measurements and City Scale Modelling to Assess the COVID–19 Lockdown Effects on Emissions and Air Quality in Athens, Greece, Atmosphere, 11, 1174, https://doi.org/10.3390/atmos11111174, 2020.

Guevara, M., Lopez-Aparicio, S., Cuvelier, C., Tarrason, L., Clappier, A., and Thunis, P.: A benchmarking tool to screen and compare bottom-up and top-down atmospheric emission inventories, Air Qual Atmos Health, 10, 627–642, https://doi.org/10.1007/s11869-016-0456-6, 2017.

Guevara, M., Jorba, O., Tena, C., Denier van der Gon, H., Kuenen, J., Elguindi, N., Darras, S., Granier, C., and Pérez García-Pando, C.: Copernicus Atmosphere Monitoring Service TEMPOral profiles (CAMS-TEMPO): global and European emission temporal profile maps for atmospheric chemistry modelling, Earth Syst. Sci. Data, 13, 367–404, https://doi.org/10.5194/essd-13-367-2021, 2021.

Hassan, S. K., El-Abssawy, A. A., AbdEl-Maksoud, A. S., Abdou, M. H., and Khoder, M. I.: Seasonal Behaviours and Weekdays/Weekends Differences in Elemental Composition of Atmospheric Aerosols in Cairo, Egypt, Aerosol Air Qual. Res., 13, 1552–1562, https://doi.org/10.4209/aaqr.2012.12.0349, 2013.

Hoyos, C. D., Herrera-Mejía, L., Roldán-Henao, N., and Isaza, A.: Effects of fireworks on particulate matter concentration in a narrow valley: the case of the Medellín metropolitan area, Environ Monit Assess, 192, 6, https://doi.org/10.1007/s10661-019-7838-9, 2020.

Hua, J., Zhang, Y., de Foy, B., Mei, X., Shang, J., and Feng, C.: Competing PM2.5 and NO2 holiday effects in the Beijing area vary locally due to differences in residential coal burning and traffic patterns, Science of The Total Environment, 750, 141575, https://doi.org/10.1016/j.scitotenv.2020.141575, 2021.

Huang, X., Ding, A., Gao, J., Zheng, B., Zhou, D., Qi, X., Tang, R., Wang, J., Ren, C., Nie, W., Chi, X., Xu, Z., Chen, L., Li, Y., Che, F., Pang, N., Wang, H., Tong, D., Qin, W., Cheng, W., Liu, W., Fu, Q., Liu, B., Chai, F., Davis, S. J., Zhang, Q., and He, K.: Enhanced secondary pollution offset reduction of primary emissions during COVID-19 lockdown in China, 10, https://doi.org/10.1093/nsr/nwaa137, 2020.

Iriti, M., Piscitelli, P., Missoni, E., and Miani, A.: Air Pollution and Health: The Need for a Medical Reading of Environmental Monitoring Data, IJERPH, 17, 2174, https://doi.org/10.3390/ijerph17072174, 2020.

Jacob, D. J. and Winner, D. A.: Effect of climate change on air quality, 43, 51–63, https://doi.org/10.1016/j.atmosenv.2008.09.051, 2009.

Jhun, I., Coull, B. A., Schwartz, J., Hubbell, B., and Koutrakis, P.: The impact of weather changes on air quality and health in the United States in 1994–2012, Environ. Res. Lett., 10, 084009, https://doi.org/10.1088/1748-9326/10/8/084009, 2015.

Jiang, Q., Sun, Y. L., Wang, Z., and Yin, Y.: Aerosol composition and sources during the Chinese Spring Festival: fireworks, secondary aerosol, and holiday effects, Atmos. Chem. Phys., 15, 6023–6034, https://doi.org/10.5194/acp-15-6023-2015, 2015.

Joly, M. and Peuch, V.-H.: Objective classification of air quality monitoring sites over Europe, Atmospheric Environment, 47, 111–123, https://doi.org/10.1016/j.atmosenv.2011.11.025, 2012.

Karl, M., Bieser, J., Geyer, B., Matthias, V., Jalkanen, J.-P., Johansson, L., and Fridell, E.: Impact of a nitrogen emission control area (NECA) on the future air quality and nitrogen deposition to seawater in the Baltic Sea region, Atmos. Chem. Phys., 19, 1721–1752, https://doi.org/10.5194/acp-19-1721-2019, 2019.

Khalil, M. A. K., Butenhoff, C. L., Porter, W. C., Almazroui, M., Alkhalaf, A., and Al-Sahafi, M. S.: Air quality in Yanbu, Saudi Arabia, Journal of the Air & Waste Management Association, 66, 341–355, https://doi.org/10.1080/10962247.2015.1129999, 2016.

Khezri, B., Chan, Y. Y., Tiong, L. Y. D., and Webster, R. D.: Annual air pollution caused by the Hungry Ghost Festival, Environ. Sci.: Processes Impacts, 17, 1578–1586, https://doi.org/10.1039/C5EM00312A, 2015.

Kouznetsov and Delgado: SILAM open code at GitHub, available at: https://github.com/fmidev/silam-model, last access: 20 October 2021.

Kouznetsov, R. and Sofiev, M.: A methodology for evaluation of vertical dispersion and dry deposition of atmospheric aerosols, 117, https://doi.org/doi:10.1029/2011JD016366, 2012.

Kouznetsov, R., Sofiev, M., Vira, J., and Stiller, G.: Simulating age of air and the distribution of SF₆ in the stratosphere with the SILAM model, Atmos. Chem. Phys., 20, 5837–5859, https://doi.org/10.5194/acp-20-5837-2020, 2020.

Kukkonen, J., López-Aparicio, S., Segersson, D., Geels, C., Kangas, L., Kauhaniemi, M., Maragkidou, A., Jensen, A., Assmuth, T., Karppinen, A., Sofiev, M., Hellén, H., Riikonen, K., Nikmo, J., Kousa, A., Niemi, J. V., Karvosenoja, N., Santos, G. S., Sundvor, I., Im, U., Christensen, J. H., Nielsen, O.-K., Plejdrup, M. S., Nøjgaard, J. K., Omstedt, G., Andersson, C., Forsberg, B., and Brandt, J.: The influence of residential wood combustion on the concentrations of PM_{2.5} in four Nordic cities, Atmos. Chem. Phys., 20, 4333–4365, https://doi.org/10.5194/acp-20-4333-2020, 2020.

Lai, Y. and Brimblecombe, P.: Regulatory effects on particulate pollution in the early hours of Chinese New Year, 2015, Environ Monit Assess, 189, 467, https://doi.org/10.1007/s10661-017-6167-0, 2017.

Lehtomäki, H., Korhonen, A., Asikainen, A., Karvosenoja, N., Kupiainen, K., Paunu, V.-V., Savolahti, M., Sofiev, M., Palamarchuk, Y., Karppinen, A., Kukkonen, J., and Hänninen, O.: Health impacts of ambient air pollution in Finland, 15, https://doi.org/10.3390/ijerph15040736, 2018.

Lonati, G., Giugliano, M., and Cernuschi, S.: The role of traffic emissions from weekends' and weekdays' fine PM data in Milan, Atmospheric Environment, 40, 5998–6011, https://doi.org/10.1016/j.atmosenv.2005.12.033, 2006.

McGraw, J., Haas, P., Young, L., and Evens, A.: Greenhouse gas emissions in Chicago: Emissions inventories and reduction strategies for Chicago and its metropolitan region, Journal of Great Lakes Research, 36, 106–114, https://doi.org/10.1016/j.jglr.2009.11.010, 2010.

Menut, L., Goussebaile, A., Bessagnet, B., Khvorostiyanov, D., and Ung, A.: Impact of realistic hourly emissions profiles on air pollutants concentrations modelled with CHIMERE, Atmospheric Environment, 49, 233–244, https://doi.org/10.1016/j.atmosenv.2011.11.057, 2012.

Menut, L., Bessagnet, B., Siour, G., Mailler, S., Pennel, R., and Cholakian, A.: Impact of lockdown measures to combat Covid-19 on air quality over western Europe, 741, 140426–140426, https://doi.org/10.1016/j.scitotenv.2020.140426, 2020.

Mues, A., Kuenen, J., Hendriks, C., Manders, A., Segers, A., Scholz, Y., Hueglin, C., Builtjes, P., and Schaap, M.: Sensitivity of air pollution simulations with LOTOS-EUROS to the temporal distribution of anthropogenic emissions, Atmos. Chem. Phys., 14, 939–955, https://doi.org/10.5194/acp-14-939-2014, 2014.

Nodehi, R. N., Hashemi, S. Y., and Azimi, F.: The effect of national events and holidays on ambi- ent pm2.5 concentrations, 3, 109–118, 2018.

Parra, R. and Franco, E.: Identifying the Ozone Weekend Effect in the air quality of the northern Andean region of Ecuador, 207, 12, 2016.

Petersen, A. K., Brasseur, G. P., Bouarar, I., Flemming, J., Gauss, M., Jiang, F., Kouznetsov, R., Kranenburg, R., Mijling, B., Peuch, V.-H., Pommier, M., Segers, A., Sofiev, M., Timmermans, R., van der A, R., Walters, S., Xie, Y., Xu, J., and Zhou, G.: Ensemble forecasts of air quality in eastern China – Part 2: Evaluation of the MarcoPolo–Panda prediction system, version 1, 12, 1241–1266, https://doi.org/10.5194/gmd-12-1241-2019, 2019.

Poupkou, A., Giannaros, T., Markakis, K., Kioutsioukis, I., Curci, G., Melas, D., and Zerefos, C.: A model for European Biogenic Volatile Organic Compound emissions: Software development and first validation, Environmental Modelling & Software, 25, 1845–1856, https://doi.org/10.1016/j.envsoft.2010.05.004, 2010.

Retama, A., Neria-Hernández, A., Jaimes-Palomera, M., Rivera-Hernández, O., Sánchez-Rodríguez, M., López-Medina, A., and Velasco, E.: Fireworks: A major source of inorganic and organic aerosols during Christmas and New Year in Mexico city, Atmospheric Environment: X, 2, 100013, https://doi.org/10.1016/j.aeaoa.2019.100013, 2019.

Rozbicka, K. and Rozbicki, T.: The “Weekend Effect” on Ozone in the Warsaw Conurbation, Poland, Pol. J. Environ. Stud., 25, 1675–1683, https://doi.org/10.15244/pjoes/61815, 2016.

Sharma, S., Zhang, M., Anshika, Gao, J., Zhang, H., and Kota, S. H.: Effect of restricted emissions during COVID-19 on air quality in India, Science of The Total Environment, 728, 138878, https://doi.org/10.1016/j.scitotenv.2020.138878, 2020.

Shi, C., Wu, H., and Chiu, Y.-H.: The Dynamic Analysis of the Pollutant Emissions Impact on Human Health in China Industries Based on the Meta-Frontier DEA, Healthcare, 8, 5, https://doi.org/10.3390/healthcare8010005, 2019.

Singh, A., Pant, P., and Pope, F. D.: Air quality during and after festivals: Aerosol concentrations, composition and health effects, 227, 220–232, https://doi.org/10.1016/j.atmosres.2019.05.012, 2019.

Singh, K. P., Gupta, S., and Rai, P.: Identifying pollution sources and predicting urban air quality using ensemble learning methods, Atmospheric Environment, 80, 426–437, https://doi.org/10.1016/j.atmosenv.2013.08.023, 2013.

Sofiev, M.: A model for the evaluation of long-term airborne pollution transport at regional and continental scales, 34, 2481–2493, 2000.

Sofiev, M.: Extended resistance analogy for construction of the vertical diffusion scheme for dispersion models, 107, ACH 10-1-ACH 10-8, https://doi.org/10.1029/2001JD001233, 2002.

Sofiev, M.: On possibilities of assimilation of near-real-time pollen data by atmospheric composition models, 1, https://doi.org/10.1007/s10453-019-09583-1, 2019.

Sofiev, M., Siljamo, P., Valkama, I., Ilvonen, M., and Kukkonen, J.: A dispersion modelling system SILAM and its evaluation against ETEX data, 40, 674–685, https://doi.org/10.1016/j.atmosenv.2005.09.069, 2006.

Sofiev, M., Genikhovich, E., Keronen, P., and Vesala, T.: Diagnosing the Surface Layer Parameters for Dispersion Models within the Meteorological-to-Dispersion Modeling Interface, 49, 221–233, https://doi.org/10.1175/2009JAMC2210.1, 2010.

Sofiev, M., Soares, J., Prank, M., de Leeuw, G., and Kukkonen, J.: A regional-to-global model of emission and transport of sea salt particles in the atmosphere, 116, https://doi.org/10.1029/2010JD014713, 2011.

Sofiev, M., Vira, J., Kouznetsov, R., Prank, M., Soares, J., and Genikhovich, E.: Construction of an Eulerian atmospheric dispersion model based on the advection algorithm of M. Galperin: dynamic cores v.4 and 5 of SILAM v.5.5, 8, 3497–3522, https://doi.org/10.5194/gmd-8-3497-2015, 2015a.

Sofiev, M., Berger, U., Prank, M., Vira, J., Arteta, J., Belmonte, J., Bergmann, K. C., Charoux, F., Elbern, H., Friese, E., Galan, C., Gehrig, R., Khvorostyanov, D., Kranenburg, R., Kumar, U., Marecal, V., Meleux, F., Menut, L., Pessi, A.-M., Robertson, L., Ritenberga, O., Rodinkova, V., Saarto, A., Segers, A., Severova, E., Sauliene, I., Siljamo, P., Steensen, B. M., Teinemaa, E., Thibaudon, M., and Peuch, V.-H.: MACC regional multi-model ensemble simulations of birch pollen dispersion in Europe, 15, 8115–8130, https://doi.org/10.5194/acp-15-8115-2015, 2015b.

Sofiev, M., Kouznetsov, R., Hänninen, R., and Sofieva, V. F.: Technical note: Intermittent reduction of the stratospheric ozone over northern Europe caused by a storm in the Atlantic Ocean, Atmos. Chem. Phys., 20, 1839–1847, https://doi.org/10.5194/acp-20-1839-2020, 2020.

Vira, J. and Sofiev, M.: On variational data assimilation for estimating the model initial conditions and emission fluxes for short-term forecasting of SOx concentrations, 46, 318–328, https://doi.org/10.1016/j.atmosenv.2011.09.066, 2012.

Wang, Q. and Su, M.: A preliminary assessment of the impact of COVID-19 on environment – A case study of China, Science of The Total Environment, 728, 138915, https://doi.org/10.1016/j.scitotenv.2020.138915, 2020.

Wesely, M. L.: Parameterization of surface resistances to gaseous dry deposition in regional-scale numerical models, 23, 1293–1304, 1989.

Xian, P., Reid, J. S., Hyer, E. J., Sampson, C. R., Rubin, J. I., Ades, M., Asencio, N., Basart, S., Benedetti, A., Bhattacharjee, P. S., Brooks, M. E., Colarco, P. R., da Silva, A. M., Eck, T. F., Guth, J., Jorba, O., Kouznetsov, R., Kipling, Z., Sofiev, M., Perez Garcia-Pando, C., Pradhan, Y., Tanaka, T., Wang, J., Westphal, D. L., Yumimoto, K., and Zhang, J.: Current state of the global operational aerosol multi-model ensemble: An update from the International Cooperative for Aerosol Prediction (ICAP), 145, 176–209, https://doi.org/10.1002/qj.3497, 2019.

Xu, Z., Huang, X., Nie, W., Chi, X., Xu, Z., Zheng, L., Sun, P., and Ding, A.: Influence of synoptic condition and holiday effects on VOCs and ozone production in the Yangtze River Delta region, China, Atmospheric Environment, 168, 112–124, https://doi.org/10.1016/j.atmosenv.2017.08.035, 2017.

Yao, L., Wang, D., Fu, Q., Qiao, L., Wang, H., Li, L., Sun, W., Li, Q., Wang, L., Yang, X., Zhao, Z., Kan, H., Xian, A., Wang, G., Xiao, H., and Chen, J.: The effects of firework regulation on air quality and public health during the Chinese Spring Festival from 2013 to 2017 in a Chinese megacity, Environment International, 126, 96–106, https://doi.org/10.1016/j.envint.2019.01.037, 2019.

Yarwood, G., Rao, S., Yocke, M., and Whitten, G. Z.: Updates to the carbon bond chemical mechanism: CB05, US EPA, 2005.

Ye, C., Chen, R., and Chen, M.: The impacts of Chinese Nian culture on air pollution, Journal of Cleaner Production, 112, 1740–1745, https://doi.org/10.1016/j.jclepro.2015.04.113, 2016.

Zhao, Y., Qiu, L. P., Xu, R. Y., Xie, F. J., Zhang, Q., Yu, Y. Y., Nielsen, C. P., Qin, H. X., Wang, H. K., Wu, X. C., Li, W. Q., and Zhang, J.: Advantages of a city-scale emission inventory for urban air quality research and policy: the case of Nanjing, a typical industrial city in the Yangtze River Delta, China, Atmos. Chem. Phys., 15, 12623–12644, https://doi.org/10.5194/acp-15-12623-2015, 2015.

Zhou, M., Jiang, W., Gao, W., Zhou, B., and Liao, X.: A high spatiotemporal resolution anthropogenic VOC emission inventory for Qingdao City in 2016 and its ozone formation potential analysis, Process Safety and Environmental Protection, 139, 147–160, https://doi.org/10.1016/j.psep.2020.03.040, 2020.

Zou, Y., Charlesworth, E., Yin, C. Q., Yan, X. L., Deng, X. J., and Li, F.: The weekday/weekend ozone differences induced by the emissions change during summer and autumn in Guangzhou, China, Atmospheric Environment, 199, 114–126, https://doi.org/10.1016/j.atmosenv.2018.11.019, 2019.